

**TREND REMOVAL FROM ELECTROCHEMICAL NOISE DATA**

Mauricio Ohanian, Víctor Martínez-Luaces, Verónica Díaz\*

Facultad de Ingeniería – UDELAR. J. Herrera y Reissig 565, C.P. 11300. Montevideo, Uruguay

***Abstract***

Three trend removal methods were performed over computational simulated data. Their performance was evaluated by sequence dependent and independent statistical analysis. Polynomial fitting, moving average removal (MAR) and moving median removal (MMR) were used for trend removal. It was concluded that the MMR method yielded the best results for the simulated signals. In order to evaluate these methods with experimental data, the electrochemical noise (EN) technique was employed to characterize – ex situ – corrosion products from low alloy steel under atmospheric corrosion conditions.

**Keywords:** electrochemical calculation; electrochemical noise; simulation

Universidad de la República. J. Herrera y Reissig 565. CP11300. Montevideo. Uruguay.

## 1 Introduction

The electrochemical noise (EN) technique measures fluctuations in potential and/or current, produced by variations in electrochemical kinetics. An advantage of this corrosion monitoring technique is that no external signals are required, so the system is characterized under free conditions. Furthermore, the apparatus is more affordable than other electrochemical techniques [1]. Application of the EN technique yields information on corrosion process mechanisms, kinetics and morphology [2] from the calculation of the parameters of noise resistance ( $R_N = \frac{\sigma_v}{\sigma_i}$ ), localization index ( $LI = \frac{\sigma_i}{I_{RMS}}$ ), and power spectral density ( $PSD$ ).

EN provides information in terms of current and potential fluctuations of low amplitude and frequency. The term 'drift' could be defined as a temporal change in the average of the measured parameters. The definition of drift is very close to that of EN: in fact, the difference between drift and EN is diffuse.

Drift implies the existence of a non-stationary signal at least within the measurement time. In these conditions, EN statistical analysis from the point of view of sequence independent (calculation of standard deviation) or sequence dependent (calculation of power spectral density) analyses becomes invalid.

Instability in the response of the test electrode during the experiment is frequently found in other electrochemical techniques such as electrochemical impedance spectroscopy (EIS). The origin of the drift is found in electrochemical phenomena with a duration that exceeds the maximum experimental time, in the diffusion of reactive or corrosion products toward or away from the interface, in the dissolution of corrosion products and in wetting phenomena.

K. Hung Chan et al [3] developed some theoretical aspects of the trend removal problem. They established the difference between the most popular trend removal methods, i.e., first differences (so-called point to point) and least square regression. The authors proved that under linear trend and white noise, the first difference filter generated an exaggerated power spectral density (PSD) at high frequency and attenuated PSD at low frequency. On the other hand, the regression residuals exhibited exaggerated PSD at low frequency and attenuated PSD in the high frequency region.

Mansfeld et al. [4] carried out a theoretical and experimental study of the effects of trends in noise fluctuations. They applied a linear fit method to the trend from experimental data. As a result, the authors obtained good agreement between the spectral noise plots after trend removal and impedance spectra determined at the same exposure time. They concluded that the moving average removal method (MAR) proposed by Tan et al. [5], generated erroneous results.

Bertocci et al. [6] analysed the performance of commonly used trend removal methods, i.e., MAR, polynomial fitting, digital high pass filtering and analogical high pass filtering. The methods were applied on simulated data obtained by overlapping white noise and linear trend. The authors examined the influence of box size on the MAR method, concluding that using a small MAR box size effectively removes the drift without phase shift, but also removes a large part of the low frequency components of the signal. On the other hand, a high order MAR method generates artefacts in the signal shape. Analysing the polynomial method, the authors presented the attenuation produced by polynomials of different orders, for different experimental periods. The 5<sup>th</sup> polynomial order was effective for the elimination of the components of frequency  $1/T$  and  $2/T$  (where  $T$  is the experimental period) but the best results were achieved when the polynomial method was combined with prepossessing windowing (Hann window). The digital Chebyshev window of different cut-off, retrieving the white noise PSD after applying a high pass (HP) filter,

was also performed. The authors considered that HP analogical filtering is the ideal way to eliminate low frequency components of the signal. However, active filters of cut-off frequency close to  $1/T$  and low intrinsic noise are too expensive. Moreover, the greatest drawback of analogical filtering in real time is that the components are subjected to large oscillations when the signal suddenly varies, such as when switching the system on.

In a previous work [7] Ohanian et al. found excessively high dispersion for experimental EN results for low alloy steel in sodium sulphate solution. They ascribed this excessive EN dispersion to the detrending data method employed. Working with simulated data they studied the influence of the polynomial detrending step and the aliasing phenomena, and they confirmed that the trend removal method employed was the principal cause of the excessive dispersion in the EN parameters. Polynomial fitting was compared with the back first differential method, Butterworth filtering (Matlab® Signal Processing Toolbox®) and a method proposed by the authors: median interval cubic splines (MICS). The MICS method, showed the best training performance. In this method a group of points (nodes) were obtained by dividing simulated data into  $n$  equal intervals, and computing the average time and position within the interval. These nodes were matched using cubic splines. Finally, noise was calculated as the difference between the simulated data and the interpolated trend.

Another method proposed in the literature utilizes Artificial Neural Networks (ANN) in connection with Data Simulators for detrending. ANN was successfully used for traditional Noise Filtering in a wide range of areas. In a previous study of ours (Martínez et al. [8], Back propagation ANN was trained with simulated data, and as a result, a good level of predictive ability was obtained in the case of Lorentz's function with Gaussian-distributed noise. Indeed, we found that in ANN detrending, especially at high frequencies, there was no influence on the superimposed signal. These results and PSD validation were published [8]. However, we found that when the degrees

of freedom increased, poor results were obtained, mainly in the low frequencies domain, in the case of trend and/or using non-Gaussian distributed noise. Moreover, with increasing difference between trend and noise, the method became less accurate. The use of ANN in real data, with non predictable trend shape, would require a variety of training curves or pre selection of the network to be used.

The aim of this work was to analyse the performance of three methods of trend removal, i.e., polynomial detrending, moving average removal (MAR), and moving median removal (MMR). The signals analysed were simulated data sets with different and non-trivial tendencies. The noise employed was a discrete transient of exponential decay that simulates a non-stationary pit. Finally, the detrending methods were also applied in order to characterize protective properties of the corrosion products formed in low alloy steel (in sodium sulphate media) exposed to atmospheric conditions in an Antarctic site [9] for one year.

## 2 Materials and methods

### 2.1 Noise simulation

Two EN data sets were generated by adding simulated noise data and two different trend lines.

In all cases the interval between data points was 0.7 seconds.

Noise: the noise consisted in a pulse train with an amplitude corresponding to a uniform distribution of [0, 2.5). Initial time was obtained from a binomial distribution of 0.02 and its sign had a binomial distribution of 0.5.

The pulse function used could be expressed as:

$$f(t) = ABt \exp(-b(t-c)^d) \quad (1)$$

Parameters  $b$ ,  $c$  and  $d$ , were adjusted in order to obtain a signal similar to a representative experimental transient. Factor  $A$  represented the amplitude and parameter  $B$  adjusted the sign function.

## 2.2 Trend simulation

Functions used as trend lines in simulation processes must be non-trivial. Polynomials, sinusoids and exponentials, among others, can be considered as trivial, because they can be easily approximated by elementary mathematical methods. This is an important issue to be considered when testing trend removal methods.

Here, we used the following curves as trend lines:

Curve 1

$$f(t) = \frac{ac^{t/3}}{\Gamma\left(\frac{t}{3} + 1\right)} - b \quad (2)$$

$$\text{Where } \Gamma(x) = \int_0^{+\infty} t^{x-1} e^{-t} dt \quad \text{Euler's Gamma function} \quad (3)$$

Curve 2

$$f(t) = y_0 + \frac{2A}{\pi} \frac{w}{4(t - x_c)^2 + w^2} \quad \text{Lorentz's function} \quad (4)$$

Two signals were obtained by the addition of noise function to curve functions: Simulated signal

1: Noise plus Curve 1; Simulated signal 2: Noise plus Curve 2.

The simulated pulse train and the simulated signals are represented in Figure 1 (a) and (b); parameters were fitted in order to obtain curves with similar power trend lines.

Simulated signals and noise spectra obtained by the maximum entropy method (MEM – 15 order, ENAnalyze® program) are presented in Figure 2. The order of the MEM method applied affects the power spectrum that is obtained. If the order is small the obtained spectrum is smooth, while with high MEM order the spectrum appears much noisier. When using the MEM with relatively low order [2], comparison of the spectra obtained by applying different detrending methods is easier. Fast Fourier Transformed (FFT) provides more reliable results, but the spectra obtained are noisy and thus the representation of PSD results in the same graphic with comparative aims, is not clearly depicted thus PSD results for FFT cannot be compared clearly with the MEM results, and are not shown in Figure 2.

### 2.3 Experimental signals

The probes – low alloy steel in flat geometry – were prepared and exposed in atmospheric conditions, according to guidelines agreed in the Atmospheric Corrosion Iberoamerican Map (Spanish acronym MICAT) project, experimental details of which can be found in the literature [9]. Specifically, the probes analysed were exposed for one year at the Uruguayan Antarctic Base (Lat: 62° 10'S, Long: 58° 50'W, Elevation: 17.2 m OSL,  $SO_2$ : <0.05 mg day<sup>-1</sup>m<sup>-2</sup>,  $Cl^-$ : 160 mg day<sup>-1</sup>m<sup>-2</sup>). For this period, the time of wetness ( $RH$ >80%, temperature> 0 °C), expressed as annual frequency, was 0.354. Corrosion penetration in the substrates, measured by a gravimetric method, was 66 µm/yr [10-11].

Finally, the corrosion products were characterized ex-situ by electrochemical methods (EN) and scanning electron microscopy (SEM).



Electrochemical runs were performed using a three-electrode compartment cell with three electrodes: saturated calomel reference electrode (SCE) with a Luggin-Haber capillary tip, working electrode (WE) and counter-electrode (CE) of low carbon steel. The temperature for all runs was  $20 \pm 2$  °C. Sodium sulphate 0.1M was employed as the supporting electrolyte.

The potential of the WE against the SCE and the current between the WE and CE were recorded every 0.7 seconds using the electrochemical interface ACM Gill8AC. Each run lasted for one hour. Potential values in the text are given on the saturated calomel reference electrode (SCE) scale.

## 2.4 Trend removal methods

Three different drift removal methods were evaluated: Polynomial fitting (9-order), MAR, and MMR.

### ➤ Polynomial fitting (9-order)

This is a widely utilised method. The trend is fitted using least squares regression. The noise is computed as the difference between experimental and predicted data (by the regression model). In this case, a nine-order polynomial was utilised. The order of the detrending polynomial allows a cut-off frequency of approximately  $1/T$  [7], in this case  $3 \times 10^{-4}$  Hz.

### ➤ MAR-10

In this method, the noise is computed as

$$x_n - m_n \tag{5}$$

where  $x_n$  denotes the n-th simulated value and  $m_n$  represents the following moving average:



$$m_n = \frac{1}{21} \sum_{p=-10}^{10} x_{n+p} \quad (6)$$

Bertocci et al. [6] presented the transfer function for MAR-p:

$$H_{\text{MAR}}(f) = 1 - \frac{1}{2p+1} \frac{\sin([2p+1]\pi f/f_s)}{\sin(\pi f/f_s)}, \quad (7)$$

where  $f_s$  represents the sample frequency. The useful frequency range, within which the spectrum is not attenuated, is between  $f_{\text{max}}/(2p+1)$  and  $f_{\text{max}}$ . The highest frequency is the Nyquist frequency ( $f_{\text{max}} = f_s/2$ ). In our case the interval used was between  $3.4 \times 10^{-2}$  and 0.7 Hz.

#### ➤ MMR-10

MMR is equal to the MAR method, except for the substitution of the moving mean by the moving median. In this method, the noise is computed as

$$x_n - k_n \quad (8)$$

where  $x_n$  denotes an experimental value and  $k_n$  represents the moving median:

$$k_n = \text{median}[x_{n-10}, \dots, x_n, \dots, x_{n+10}] \quad (9)$$

### 3 Results and discussion

**3.1 Simulated signals** The Simulated Noise data set had a mean of  $-0.0112$  and standard deviation of  $0.3736$ . *Table 1* shows the statistical results for the trend removal methods employed for simulated signals 1 and 2.

With all the methods performed, the noise mean value reported was close nearby to zero (*Table 1*). Consequently, it was not possible to come to any conclusions about the performance of the drift removing methods taking only this parameter into consideration.

Figure 2 shows the spectra of the simulated signal, the original simulated noise and those obtained for the detrending methods employed.

The simulated noise data presented a spectrum with white noise in the low frequency region with amplitude 0.5. This value is coincident with the transient mean amplitude. At 0.04 Hz the spectra had a break point, the linear shape has a slope of -2.6 dec/dec (roll-off slope). The frequency of the break point calculated according to Cheng et al. [14] was 0.08 Hz (inverse of  $2 \cdot \pi \cdot \text{transitory period}$ ) and the PSD break point was 0.2 ( $2 \cdot \pi \cdot \text{initiation rate} \cdot \text{mean amplitude} \cdot \text{transitory period}$ ).

#### ➤ 9-order polynomial

The standard deviations are presented in *Table 1*. For Signal 1 – with a smoother trend – the standard deviation is close to the original noise dispersion. For Signal 2, the method gives a standard deviation greater than the original one.

The spectra confirm this behaviour: for Signal 2 the polynomial method does not remove the power in the low frequency region. The spectrum obtained for Signal 1 is a good reproduction of the trace of the original simulated noise. Thus, it is clear that this detrending method is strongly dependent on the simulated trend curve, and in contrast to what has been stated by other investigators in recent published papers [6], in the conditions of this study, we found it was not a reliable pre-processing method.

#### ➤ MAR-10

This method was not significantly dependent on the trend curve employed (Table 1). In fact, the standard deviation of the data was not very different from that of the simulated noise. Analysing the spectrum it can be stated that the noise obtained fit rather well to the original noise at high frequencies. However, for lower frequencies (below 0.01 Hz), there was a maximum at ca 0.07 Hz and a plateau was reached, with smaller power values than the original noise. The frequency breakpoint value obtained after processing the original noise spectrum data with the MAR method was larger than that predicted by the interval from the transfer function (7). Summing up, the spectrum recovered by MAR-10 produced a lower standard deviation value than the original data.

➤ MMR-10

In comparison with the polynomial method, both the MMR and the MAR methods were robust to the type of signal processing. The standard deviation obtained by MMR was much closer to the original values than that obtained by the MAR method. The difference between the original value and that obtained by MMR was lower in the case of Signal 1 than in the case of Signal 2. The spectra obtained fit better to the original noise than that obtained by MAR-10 in all the frequency range.

The mean is the most commonly reported statistic of location. However, extreme values will have great influence on it. The mean may not be the most appropriate statistic if there is one value that is much larger or smaller than the other values in a sample [12].

For the calculation of the median, the data must be ordered from the highest to the lowest value. This can be quite time consuming for a large data set and thus calculating the median is computationally more troublesome than calculating the mean for a data set. On the other hand, the median is unaffected by a single (or even several) very large or small numbers [13]. This characteristic is very important when approximating the tendency in an EN data set. In effect,

MMR provides a better baseline representation, and then the subtraction preserves the signal trace, with less attenuation than subtraction of the mean.

For probability distributions having an expected value and a median, the mean and the median can never differ from each other by more than one standard deviation. To express this in mathematical notation, let  $\mu$ ,  $m$ , and  $\sigma$  be respectively the mean, the median, and the standard deviation.

$$|\mu - m| \leq \sigma \quad (10)$$

$$\mu - \sigma \leq m \leq \mu + \sigma \quad (10')$$

Besides in the previous inequality, and applying the z-transform, the transfer function is limited by:

$$H_{\text{MMR}}(f) = 1 - \left( \frac{1}{2p+1} \pm \frac{1}{\sqrt{2p+1}} e^{-2p\pi f/f_s} \right) \frac{\sin([2p+1]\pi f/f_s)}{\sin(\pi f/f_s)} \quad (11)$$

The MMR transfer function has two real roots. Figure 3 shows the transfer function for the MMR-10 (grey line) and MAR-10 (black continuous line) methods. Transfer function has a characteristic cut-off frequency of 0.04 Hz for MMR-10 and 0.07 Hz for MAR-10. MMR transfer function presented negative values below 0.020Hz, and a strong oscillation nearby 0.7Hz.

### 3.2 Experimental Signals

Figure 4 shows experimental electrochemical results for current and potential. Electrochemical *ex situ* analysis were performed in probes that were exposed in atmospheric conditions. The current

data present a trend line – originated by the differences between the two 'nominally equal' electrodes– with maxima and values in the range of 0.015 to 0.04 mA. This trend line has superimposed meta stable pits. The mean pit amplitude is ca. 0.002 mA and their duration is approximately 3 seconds; their frequency is about every 25 seconds. The pits have a shape with fast birth and slow decline. The slant of the pit signals is remarkable, and is clear evidence of surface differences between the electrodes (asymmetry of electrodes).

The potential curve was smoother than the current signal and presented a decay trend line from ca. -350 mV to -500 mV vs. SCE at one hour, similar to signal 1. The amplitude of the voltage noise with respect to the corresponding signal is significantly lower than that observed in the current signal. Rust wetting and its corresponding transformation may have been the origin of this voltage tendency. The potential under -250 mV vs. SCE (an arbitrary limit, taking into account the evolution of hydrogen in normal conditions about the cathodic reaction), indicated that the rust formed was not a protective barrier against the corrosion process. The potential transient had an amplitude of ca. 0.1 – 0.5 mV.

Figure 5 shows the spectral density of the experimental data set for (a) the current and (b) the potential and the spectra for polynomial, MAR and MMR treatments.

Ignorance of the 'real' noise makes the analysis of experimental signals difficult. From the shape and amplitude of the current transients, a white noise of amplitude between  $4 \times 10^{-6}$  and  $2.5 \times 10^{-5}$  A in current spectra could be predicted. In the same way, a break point close to 0.04 - 0.2 Hz could be expected. From potential spectrum analysis, a white noise with a power of 1 mV and a similar break point could also be predicted. Analysing the poor protection of the rust formed (potential close to -400 mV vs SCE and SEM microphotographs, Figure 6), the surface would be expected to have a low polarization resistance.

The noise obtained by polynomial regression exhibited one plateau below 0.002 Hz and another above approximately 0.08 Hz. The first break point corresponded to oscillations of ca. 500 seconds. It was not clear whether these oscillations corresponded to noise or to a tendency. Their duration and triangular shape means they are unlikely to have arisen from an electrochemical phenomenon.

The second break point, 0.08 - 0.1 Hz, agrees approximately with the break point of the MAR10 and MMR10 treated data, corresponding to the mean transient duration. Below this frequency value the MMR10 and MAR10 methods exhibit spectra with amplitude lower than the high frequency plateau (common to all spectra). The interval of the MAR-10 and MMR-10 detrending methods employed was 15 seconds. The pits with duration of less than 15 seconds remained unaffected by both detrending methods. The data results corresponding to pits with duration of over 15 seconds, showed an altered shape, with diminished amplitude. This phenomenon is reflected in the attenuated spectra at below 0.1 Hz for both methods. Transients separated by less than 15 seconds. This shows the importance of the cut-off frequency selected when analysing electrochemical processes.

In the voltage spectrum the polynomial method exhibited the same performance as was observed after processing the current signal. However, there was a difference in the trend shape with respect to the treatment in the current signal. The trend in the voltage spectrum was smooth and similar to that represented in signal 1. Besides, the polynomial method gave excellent results with the simulated signal. Thus we would predict that the spectrum and the corresponding SD obtained with the polynomial treatment are close to the 'real' situation. For the MAR and MMR methods, the PSD obtained were similar to those associated with current data processing, with one unique characteristic. They depicted a signal response which was attenuated in the 0.1 – 0.5

Hz region, with the MMR PSD being lower than that obtained by the MAR method. The reason may be attributed to the low signal to noise ratio.

Table 2 shows the results of the noise resistance, the ratio of the standard deviation of voltage and current after the detrending processing with polynomial, MAR10 and MMR10. In the same table the results for MAR20 and MMR20 are shown.

$$R_N = \frac{\sigma_v}{\sigma_i} \quad (12)$$

In order to decrease the attenuation at low frequencies, detrending processes of major step were performed, i.e. MMR-20 and MAR-20, with cut off 0.025 and 0.04 Hz respectively (see Figure 7). In Figure 8 current and voltage signals processing with MMR-20 were showed.

The change in the cut off method was reflected in the increment of standard deviation of current and voltage. The deviation ratio,  $R_N$ , was not affected.

## 4 Summary

Stationary electrochemical noise data is required for the calculation of valid standard deviation and PSD. The trend removal method used affected the processed results. The ideal method should recover most of the signal information without introducing external effects.

The polynomial fitting method has a strong dependence on the trend and presents very good results for smooth tendencies. However; it exhibits rather poor performance in curves with sudden changes of slope and convexity.



The MAR method has robust results with respect to the type of curve analysed. On the other hand, this method alters the low frequency zone of spectra, and consequently the standard deviation results are not accurate. The proposed method, MMR, exhibits a better performance in the simulated signals analysed, however it has the same behaviour as the MAR method in the low frequency zone of spectra.

Based only on the experimental signals, it is not yet possible to establish strong conclusions. It is clear that the polynomial method is not a reliable trend removal technique. On the other hand, MAR and MMR treatments do not offer a definitive solution. In fact, the results suggest that the application of these methods produces an apparently attenuated response with low noise signals. In the case of the MMR method, increasing the order of magnitude was not able to improve its performance in the cases studied.

## 5 Acknowledgments

We thank Dr M.E. Martins, Dr Zinola and Dr. V. M. Dee for helping in the revision of the manuscript.

## 6 References

- [1] JR Kearns, JR Scully, PR Roberge, DL Reichert, JL Dawson, Electrochemical Noise Measurements for Corrosion Applications. ASTM, West Conshohocken, USA, 1996
- [2] R A Cottis, Interpretation of Electrochemical Noise Data, Corrosion (2001) 265:285
- [3] K Hung Chan, JC Hayya, JK Ord, A note on trend removal methods: the case of polynomial regression versus variate differencing, Econometrica (2001) 737:744

- [4] F Mansfeld, Z Sun, CH Hsu, A Nagiub, Concerning trend removal in electrochemical noise measurements, *Corr Sci.* (2001) 341:352
- [5] YJ Tan, S Bailey, B Kinsella, Factors affecting the determination of electrochemical noise resistance, *Corrosion* (1996) 469:475
- [6] U Bertocci, F Huet, RP Nogueira, P Rousseau, Drift removal procedures in the analysis of electrochemical noise, *Corrosion* (2002) 337:347
- [7] M Ohanian, V Martínez-Luaces, G Guineo-Cobs, *The Journal of Corrosion Science and Engineering*, (2004) in <http://www.jcse.org/viewpreprint.php?vol=7&pap>. Accessed 14<sup>th</sup> September 2008
- [8] M Martínez, V Martínez, M Ohanian., Data Simulation, Preprocessing and Neural Networks applied to Electrochemical Noise studies. *WSEAS Transactions: Computer Science and Applications Journal* (2006) 810:817
- [9] M Ohanian et al., Productos de corrosión formados en ambiente marino: vinculación de variables estructurales y potencial de corrosion, *Rev. Metal. Madrid* (2004) 175:185
- [10] M Morcillo, E Almeida, B Rosales, J Uruchurtu, M Marrocos (eds): *Corrosión y Protección de Metales en las Atmósferas de Iberoamérica – Parte I-Mapas de Iberoamérica de corrosividad atmosférica*. CYTED, España, 1999
- [11] ISO 9226 'Corrosion of metals and alloys Corrosivity of atmospheres Determination of corrosion rate of standard specimens for the evaluation of corrosivity'; ISO, Genève, Switzerland, 1992
- [12] On line document
- D Moore, Measures of Location Chapter 3

<http://academic.emporia.edu/mooredwi/rda/notes3.htm>. Accessed 28th july 2008

- [13] RL Scheaffer, JT McClave : Probability and Statistics for Engineers Third Edition, PWS-KENT Publishing Company, USA, 1990
  
- [14] YF Cheng, JL Luo, M Milmott, "Spectral analysis of electrochemical noiser with different transient shapes", Electrochim Acta (2000) 1763:1771

## Figure Captions

Figure 1 (a) Computationally simulated signals, obtained for superposition of pulse train (simulated noise) on Curve 1 (black line) and Curve 2 (gray line) (b) Detail of the shape of individual simulated transitory

Figure 2 PSD of simulated signal, simulated noise, and signal treated with polynomial, MMR10 and MAR10 methods. (a) Simulated signal 1: Noise + Curve 1.  
(b) Simulated signal 2: Noise + Curve 2

Figure 3 Transfer function limits for MMR-10 (grey lines), and MAR-10 transfer function (black line).

Figure 4 Time course of experimental current (black line) and potential (grey line) of EN signals

Figure 5 PSD of experimental untreated signal and signal treated with polynomial, MMR10 and MAR10 methods for (a) Current data (b) Potential data

Figure 6 SEM images at 500X and 1000X magnification.

Figure 7 Transfer function for MMR-20 (grey line) and transfer function for MAR-20 (black line)

Figure 8 Current and voltage experimental signals processing with MMR20

## Tables

*Table 1* Mean and standard deviation for trend removal methods: MAR-10, MMR-10 and 9-order polynomial fitting under simulated pulse train noise (mean: -0.0112, standard deviation: 0.3736)

	MAR-10		MMR-10		Polynomial	
Signal	Mean	SD	Mean	SD	Mean	SD
1	$2.49 \times 10^{-4}$	0.3204	$8.50 \times 10^{-3}$	0.3600	$-1.39 \times 10^{-5}$	0.3735
2	$-2.93 \times 10^{-4}$	0.3204	$5.90 \times 10^{-3}$	0.3550	$4.13 \times 10^{-3}$	1.8261

NOTA: SD is standard notation for "standard deviation"

*Table 2* Standard deviation for current and voltage and  $R_n$  for experimental signal after applying polynomial, MAR10 and MMR10 detrending methods.

	MAR10	MMR10	Polynomial	MAR 20	MMR20
$\sigma I$ (mA/cm <sup>2</sup> )	$3.40 \times 10^{-4}$	$3.40 \times 10^{-4}$	$5.82 \times 10^{-4}$	$3.57 \times 10^{-4}$	$3.47 \times 10^{-4}$
$\sigma v$ (mV)	0.0664	0.0573	0.155	0.0700	0.0573
$R_n$ ( $\Omega$ .cm <sup>2</sup> )	195	168	267	196	165

Figure1 (a)

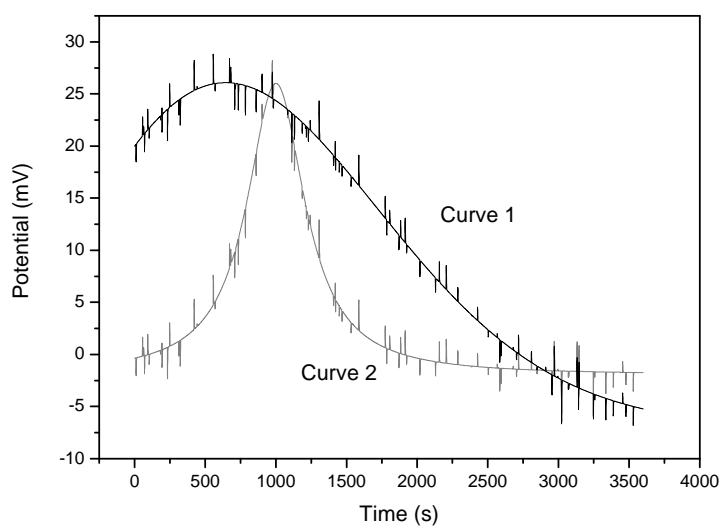


Figure1 (b)

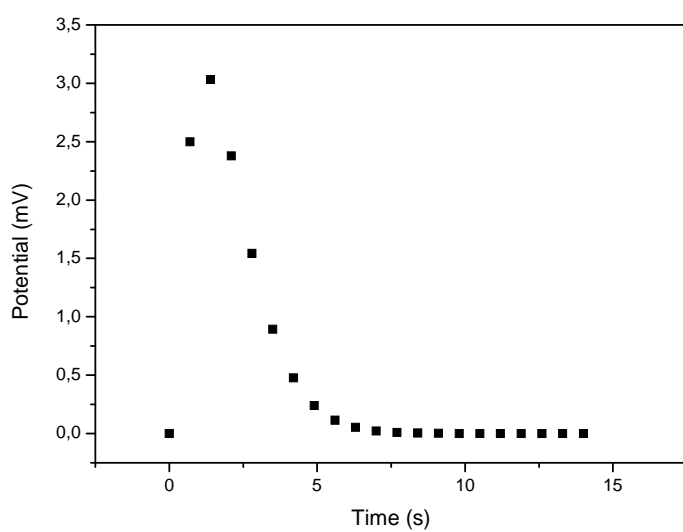


Figure 2 (a)

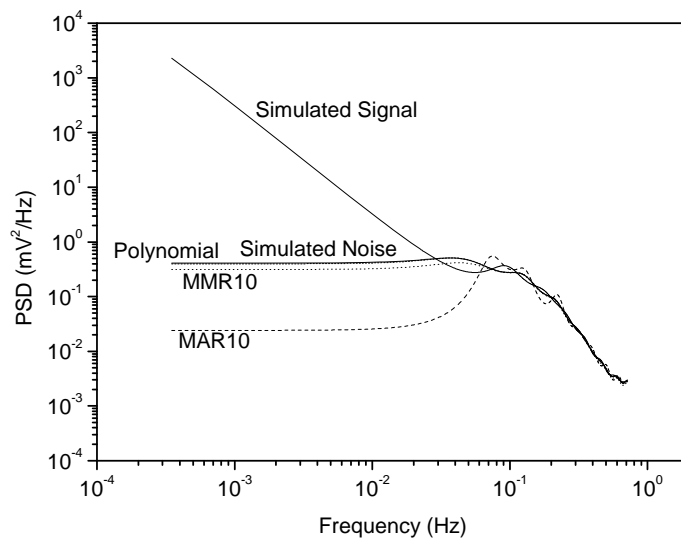


Figure 2 (b)

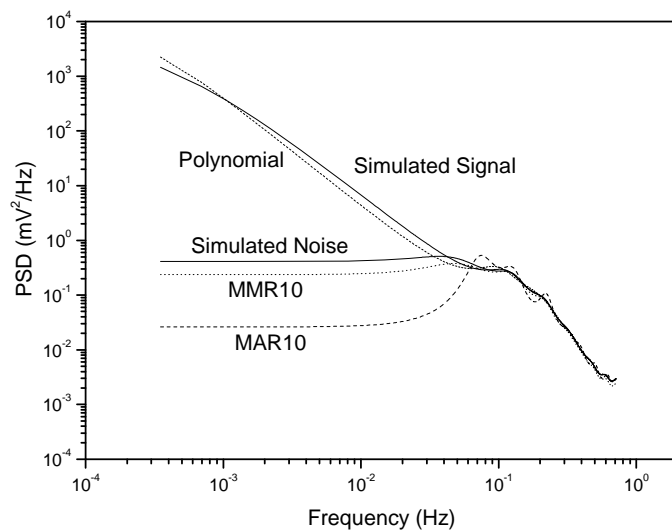






Figure 3

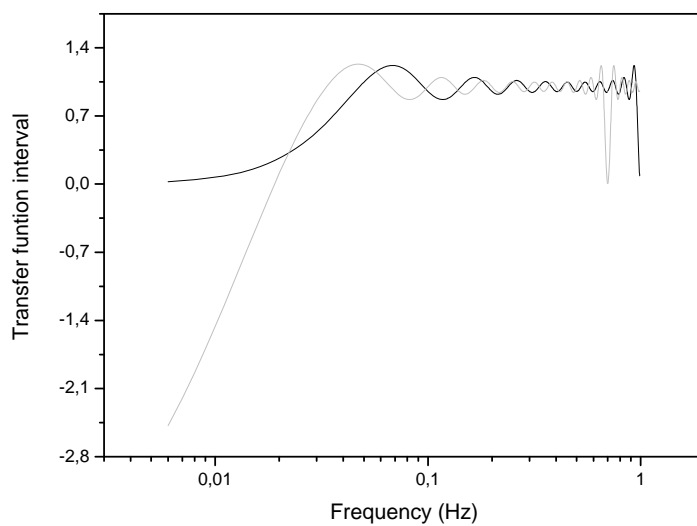


Figure 4

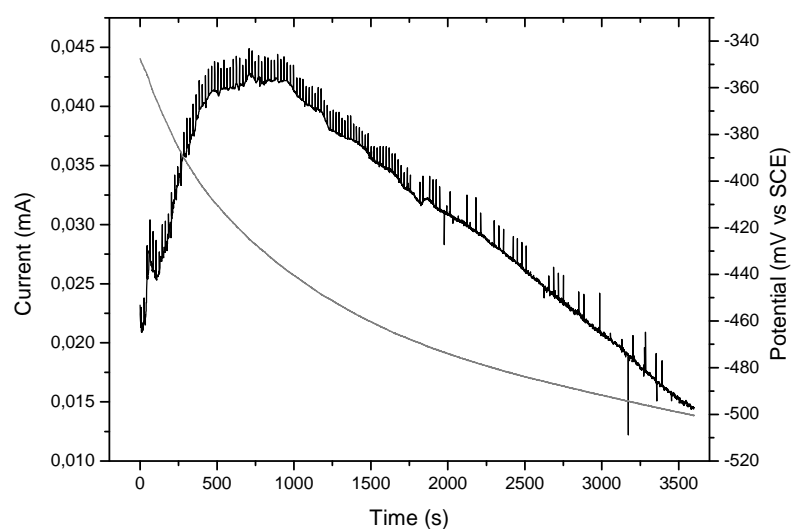


Figure5 (a)

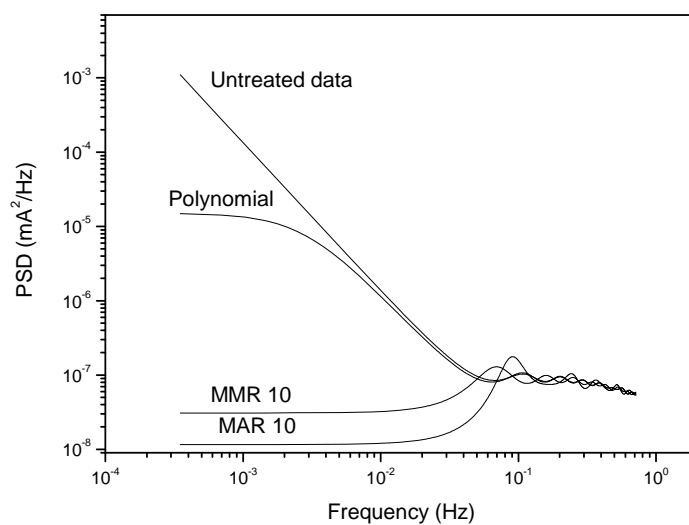


Figure5 (b)

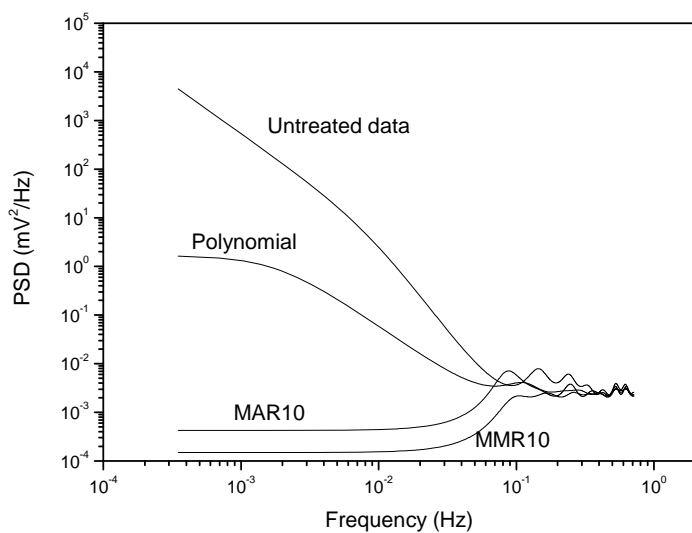


Figure 6

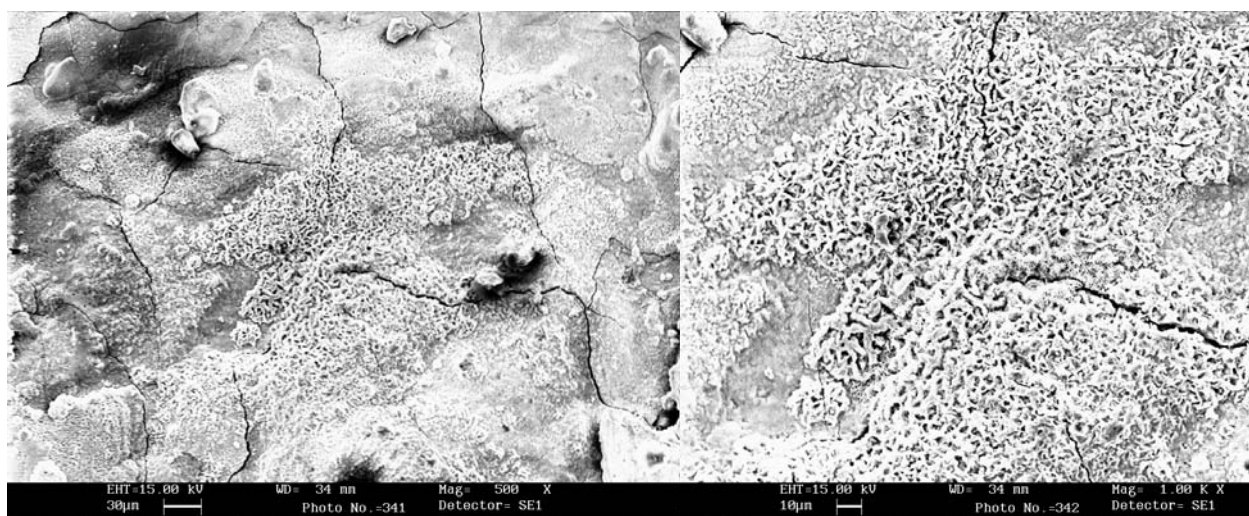


Figure 7

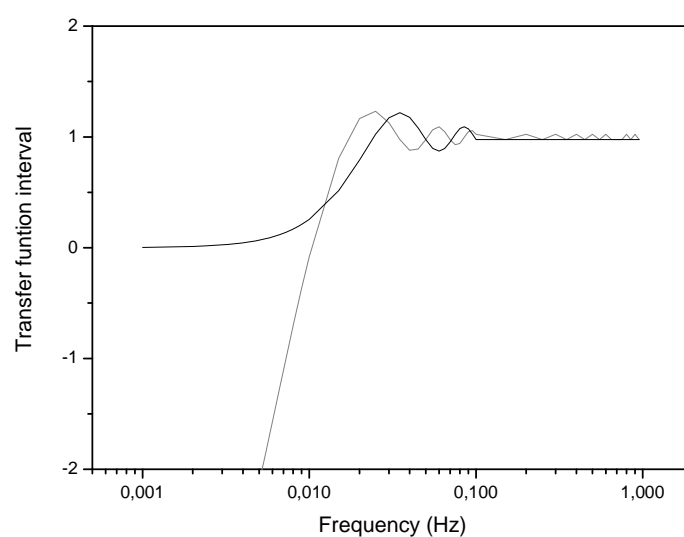


Figure 8

